

# A Bipedal Running Robot with One Actuator per Leg

Neil Neville

*Centre for Intelligent Machines  
McGill University  
Montreal QC Canada H3A 2A7  
neville@cim.mcgill.ca*

Martin Buehler

*Boston Dynamics  
515 Massachusetts Ave.  
Cambridge MA USA 02139  
buehler@bostondynamics.com*

Inna Sharf

*Centre for Intelligent Machines  
McGill University  
Montreal QC Canada H3A 2A7  
inna.sharf@mcgill.ca*

**Abstract** - This paper presents experiments with a new, three-dimensional bipedal running behaviour for our Robotic Hexapod, RHex. The robot and the bipedal gait are under-actuated, using only one actuated degree of freedom per compliant leg. We doubled up RHex's hind legs by attaching a duplicate set of hind legs at  $180^\circ$ , forming 'S' shaped legs. This reduces the actuator speed requirements during non-contact, while preserving the bipedal dynamics and control challenges. Stable running at average speeds between 0.67 and 1.07 m/s with a success rate of 100% over thirty runs is obtained with only leg angle and body orientation feedback.

**Index Terms** – bipedal running, compliance, legged robot.

## I. INTRODUCTION

One need only look at the extraordinary range of mobility present across the animal kingdom to appreciate the immense potential for legged robots in unstructured environments. Many application domains of robots also require high mobility. Such applications include fire fighting, first response, mobile monitoring, inspection and surveillance, planetary exploration, homeland security, to name just a few. Still further applications for legged robots include entertainment robots, such as toys and theme park versions of movie creatures. To address these needs, engineers have designed a huge array of robots with wheels, tracks, various numbers of legs, and combinations of wheels, tracks, and legs.

Naturally, legged robots may benefit from the inspiration of millions of years of biological evolution. This is the case with RHex, a hexapod robot inspired by research on cockroach locomotion [3, 4] with its sprawled posture, low center of gravity, passive compliant legs, and clock-driven tripod gaits. These biologically motivated ideas, combined with sound scientific and engineering principles, have endowed RHex with a large repertoire of gaits, including walking over highly broken and irregular terrain [17], pronking [10], stair climbing [11, 12], swimming [19], flipping [18], and quadrupedal bounding [2].

In this paper we describe further progress, building on our initial results [13], towards a new behaviour in RHex's already large behavioural repertoire: bipedal running. Just as the overall robot design was inspired by R.J. Full's research on cockroach locomotion, so is this particular behaviour. Full and Tu [4] reported that the American cockroach, *Periplaneta americana* (mass < 1 g) can run bipedally on its hind legs at high speeds.



Fig. 1: RHex in outdoor rock field

Why create a bipedal gait for a hexapod robot? We are interested in expanding RHex's behavioural repertoire and investigating and exploiting possible mobility, speed or energetic advantages. For example, we expect a mobility improvement in terms of step and pipe traversal heights, due to the raised centre of mass of a bipedal RHex. Furthermore, the reported behaviour is a proof of concept for a bipedal running gait with a minimal number of actuators. To our knowledge, no robot has been able to demonstrate dynamic bipedal running with just two actuators.

In recent years there has been a particular emphasis on bipedal robot research, humanoid robot research in particular [eg., 6, 7, 8, 9, 14, 16]. By and large, such bipedal robots have large feet, use a relatively high number of actuated degrees of freedom, walk slowly, are limited to the sagittal plane, or lack compliance, a notable exception being Raibert's 3D biped [15], a 6 actuator robot. Thus, the work presented in this paper emphasizes simplicity and is in strong contrast to the approach employed in the majority of biped robot projects presented in the literature in terms of actuation and sensing.

## II. PLATFORM

RHex [17] is a power-autonomous hexapod with a simple mechanical design featuring compliant legs with one actuated degree of freedom per leg. Leg retraction is accomplished by rotating the leg over the hip to avoid toe stubbing and to clear obstacles. The simplicity of the system has resulted in a robust platform for studying legged locomotion that is also a promising candidate for many practical applications. Some key physical characteristics of RHex are given in Table 1.

TABLE 1: BASIC RHEX DATA

|   |                     |          |
|---|---------------------|----------|
| Body Mass                                     | $m_b$               | 8.4 kg   |
| Leg Mass                                      | $m_l$               | 0.08 kg  |
| Body Length                                   | $l_b$               | 0.51 m   |
| Body Height                                   | $h_b$               | 0.14 m   |
| Leg Length (unloaded)                         | $l_l$               | 0.17 m   |
| Leg Spring Constant<br>(linear approximation) | $k_l$               | 1640 N/m |
| Maximum Hip Torque<br>(intermittent only)     | $\tau_{\max}$       | 5 Nm     |
| Maximum Hip Speed                             | $\dot{\phi}_{\max}$ | 5 rev/s  |

In the bipedal running, the focus of our discussion here, the front four legs of the robot are not used. To date, the development of the bipedal gait for RHex has been conducted by using modified hind legs. In particular, we modified the hind legs as follows: we attached an additional, identical half-circle shaped leg to each of the two hind legs, with a 180° offset, as can be seen in the photograph (side view) in Fig. 2. This “S” shape modification reduces the actuator speed requirements when not in stance, but otherwise does not fundamentally change the dynamics or control challenges of the system.

### III. SENSING

The control strategy uses minimal feedback – the left and right leg angles with respect to the body  $\phi_l$ ,  $\phi_r$ ; body pitch angle,  $\theta$ ; and body yaw angle,  $\psi$ . Incremental optical encoders attached to the hip actuators measure the angles of the rear legs. The body pitch, roll, and yaw angles are measured via integration of angular rates from a three-axis fiberoptic gyroscope; however, the roll angle is not used for control. The most significant sensing challenge is the absence of a forward velocity sensor. Instead, we use a low pass filtered version of the *desired* leg sweep velocity as an estimate of the actual forward velocity, as discussed in the following section. Actual forward velocity, body COM coordinates, leg lengths and angles after bending, leg forces, leg touchdown and lift-off events, are all not easily measurable and were not available.

### IV. CONTROL

The controller employed for the bipedal gait of RHex is hierarchical, with four levels of proportional derivative (PD) controls for speed control, pitch control, leg trajectory tracking, and steering. The primary motivation for PD controllers for this application is that they allow for an intuitive understanding of the control parameters that facilitates parameter tuning based on experimental data. The elements of the overall block diagram of the controller in Fig. 3 are described in the following subsections.



Fig. 2: High speed video frame during single support.

#### A. Speed P Control

The robot acts like an inverted pendulum in the sagittal plane. The speed control law,

$$\theta_d = \text{sat} \left[ k_{vp} (\bar{v} - v_d) \right] + \theta_b, \quad (1)$$

generates the desired pitch angle,  $\theta_d$ , which is an input for the inverted pendulum PD balancing controller. In the above,  $v_d$  is the desired forward velocity of the robot body (at the midpoint between the hips),  $\bar{v}$  is an estimate of the actual forward speed,  $k_{vp}$  is a proportional gain, and  $\theta_b$  is the balance angle. The desired lean angle,  $\theta_d - \theta_b$ , is limited to approximately  $\pm 6^\circ$  with a saturation function. The balance angle,  $\theta_b$ , is constant and is the pitch for which the robot has approximately zero net forward acceleration over a stride. Commanding positive lean angles will increase the robot speed and vice versa. Since both speed and body pitch need to be controlled simultaneously, but only one control input to the robot is available via the desired leg speed,  $\dot{\phi}_d$ , the speed control is set such that it responds more slowly than the more important inverted pendulum balancing controller.

#### B. Inverted Pendulum PD Control

In the sagittal plane the pitch angle is controlled via a linear PD control that calculates the desired leg stance accelerations,  $\ddot{\phi}_d$ :

$$\ddot{\phi}_d = k_{\theta p} (\theta - \theta_d) + k_{\theta d} (\dot{\theta} - \dot{\theta}_d). \quad (2)$$

In the above,  $k_{\theta p}$  and  $k_{\theta d}$  are gains, and  $\dot{\theta}_d$  is calculated online as a numerical derivative of the desired pitch angle commands from the speed P control of (1).

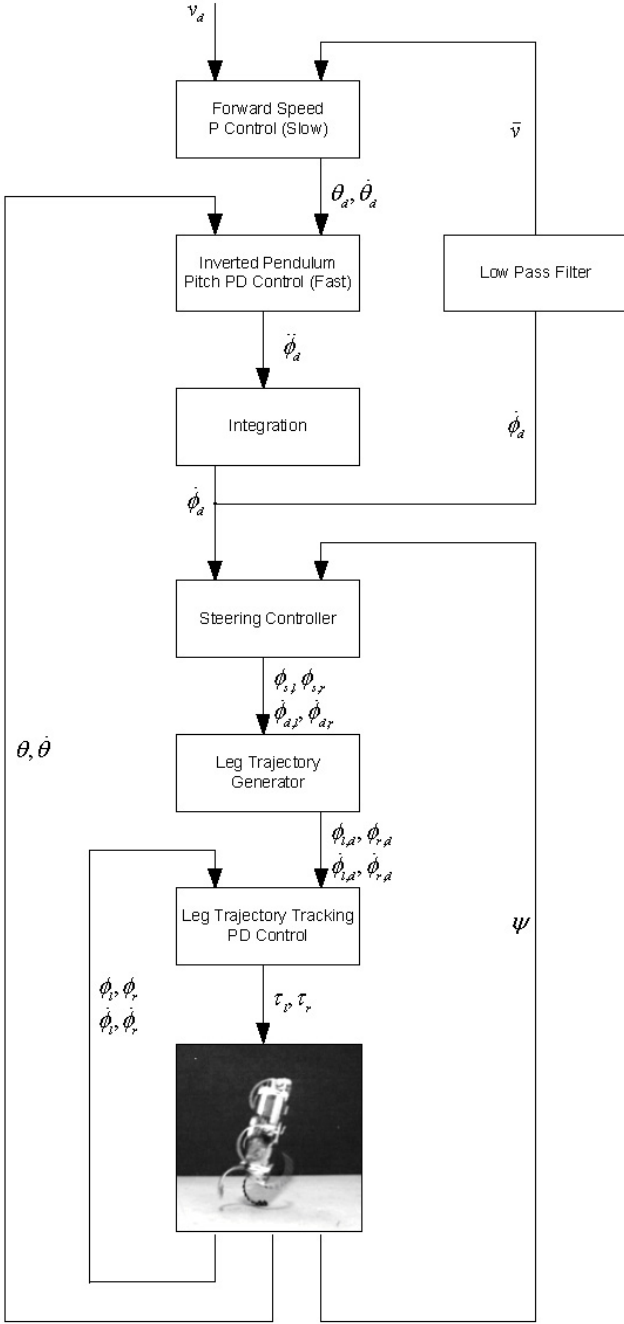


Fig. 3: Control block diagram

### C. Low Pass Filter

The forward velocity of the robot is estimated using a low pass filtered version of the leg sweep velocity,  $\bar{\phi}_d$ :

$$\bar{\phi}_d(k) = \alpha_\phi \dot{\phi}_d(k) + (1 - \alpha_\phi) \dot{\phi}_d(k-1), \quad (3)$$

where,  $\alpha_\phi$  is a parameter of the filter related to its time constant by  $t_{\phi,IR} = -T/\ln(1 - \alpha_\phi)$  and  $T$  is the sampling time. Based on the above, and an appropriate choice of filter time constant, the forward velocity estimate used by the speed

P control law is  $\bar{v} = \bar{\phi}_d l_{ave}$ . The average leg length,  $l_{ave}$ , is determined empirically.

### D. Integration

The desired leg stance speed is obtained via integration of the desired leg stance acceleration and the current leg stance speed estimate, via

$$\dot{\phi}_d = \ddot{\phi}_d + \dot{\phi}_d T, \quad (4)$$

### E. Leg Trajectory Generator

The leg trajectory generation scheme is similar to that of the RHex hexapedal tripod gait [17], which consists of open loop target trajectories parameterized by four leg trajectory parameters. In the current work, the four leg trajectory parameters used are the stance sweep angle  $\phi_s$ , the leg trajectory offset with respect to the body  $\phi_o$ , the sweep velocity  $\dot{\phi}_d$ , and the duty factor  $\beta$ . The duty factor is defined as the fraction of the leg cycle time spent in stance. In a single cycle, both legs go through their slow stance phase and fast swing phase, covering  $\phi_s$  and  $\pi - \phi_s$ , respectively.

The sweep angle,  $\phi_s$ , is set to be a linear function of the desired stance velocity,  $\dot{\phi}_d$ . The offset is a function of the pitch of the robot,  $\phi_o = \theta + C_1$ , where  $C_1$  is a constant. Together, the sweep angle and offset determine the angle of the legs when the assumed touchdown and lift-off events occur.

The duty factor determines the fraction of the cycle for which double leg support is assumed,  $(2\beta - 1)$ . During this time both legs are in their slow phases, but may not be in contact with the ground. The duration of single leg support is a key factor that determines the roll oscillation amplitude, as discussed in Section V.

The clock driven leg trajectories are updated in a 667 Hz (nominal) control loop. The commanded leg positions and velocities are based on a normalized time,  $c$ , which maps a cycle period onto the unit interval. The cycle period is given by

$$t_c = \frac{\phi_s}{\dot{\phi}_d \beta}. \quad (5)$$

Four phases are created based on the normalized time. In the case of constant leg trajectory parameters, there is a constant velocity stance phase followed by a standard three-part trapezoidal velocity profile as shown in Fig. 4. The constant high velocity phase is characterized by the maximum leg velocity and exists only when the leg trajectory requires it. The trajectory parameters are updated every sampling period. The resulting trajectories are smooth by virtue of the fact that the rate at which the trajectories are recalculated is sufficiently high. The two legs are kept 180° out of phase by a cycle time offset of 0.5 between the legs.

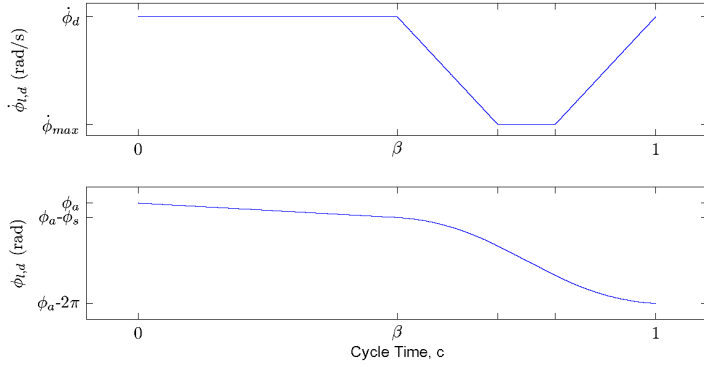


Fig. 4: Leg position (top) and velocity (bottom) trajectories for constant leg trajectory parameters and RHex legs, where  $\phi_a = \phi_s/2 + \phi_o$ .

### F. Steering Controller

Steering, or yaw angle control, is accomplished by a differential modification of the leg trajectory parameters between the two legs, such that the stride period,  $t_c$ , is maintained by both the left and right leg. This ensures that the relative phase between the legs is maintained.

The wide hip spacing of the robot results in a significant stride-to-stride yaw oscillation of up to  $6^\circ$  in amplitude with a period equal to  $t_c$ . Because this yaw angle oscillation is superimposed on the yaw angle defining the forward direction of the robot, some measure of the forward direction of the robot is required. To this end, the measured yaw angle is filtered using a low pass single pole filter, producing  $\bar{\psi}$ :

$$\bar{\psi}(k) = \alpha_\psi \psi(k) + (1 - \alpha_\psi) \psi(k-1), \quad (6)$$

where,  $\alpha_\psi$  is a parameter of the filter related to its time constant by  $t_{\psi, IIR} = -T/\ln(1 - \alpha_\psi)$ . The desired left and right leg sweep velocities,  $\dot{\phi}_{d,l}$  and  $\dot{\phi}_{d,r}$ , are modified by a fraction,  $\Delta$ :

$$\Delta = \text{sat} \left[ k_{\psi p} (\bar{\psi} - \psi_d) \right] \quad (7)$$

$$\begin{aligned} \dot{\phi}_{d,l} &= (1 + \Delta) \dot{\phi}_d \\ \dot{\phi}_{d,r} &= (1 - \Delta) \dot{\phi}_d \end{aligned} \quad (8)$$

where  $k_{\psi p}$  is the proportional gain and  $\psi_d$  is the desired yaw angle. The left and right stance sweep angles,  $\phi_{s,l}$  and  $\phi_{s,r}$ , are then modified such that both legs maintain the correct cycle time:

$$\begin{aligned} \phi_{s,l} &= \dot{\phi}_{d,l} \beta t_c \\ \phi_{s,r} &= \dot{\phi}_{d,r} \beta t_c \end{aligned} \quad (9)$$

For some experiments, including those presented in this paper, an additional term proportional to the lateral deflection was added to (7).

### G. Leg Trajectory PD Control

The desired left and right leg trajectories are tracked with a PD controller. The leg tracking controller generates desired left and right hip torques,  $\tau_{d,l}$  and  $\tau_{d,r}$  via

$$\begin{aligned} \tau_{d,l} &= k_{\phi p} (\phi_{l,d} - \phi_l) + k_{\phi d} (\dot{\phi}_{l,d} - \dot{\phi}_l) \\ \tau_{d,r} &= k_{\phi p} (\phi_{r,d} - \phi_r) + k_{\phi d} (\dot{\phi}_{r,d} - \dot{\phi}_r) \end{aligned} \quad (10)$$

The leg tracking gains,  $k_{\phi p}$ ,  $k_{\phi d}$  introduce a pose dependent compliance in series with the leg compliance and thus affect the dynamics of the gait. Since voltage controlled amplifiers are used, desired hip motor voltages are calculated from the desired torques using a simple motor model.

## V. EXPERIMENTS

### A. Method

Experimental results were produced by running the robot repeatedly over a test track consisting of a standard linoleum floor marked with 2 m wide retro-reflective tape lines spaced 5 m apart. Suitable initial conditions were provided by manually starting the robot in an upright posture with an initial velocity at a distance of approximately 2 m from the start line. The robot senses the start and end reflective tape lines via a downward facing infrared (IR) sensor and records time data required for the calculation of the actual average forward speed, average power, and total estimated lateral displacement.

Simple pragmatic criteria are used to assess stability. If the robot falls, the test is recorded as a fall failure. If the estimated forward velocity error is greater than 15% at the finish line, the trial is recorded as a speed controller failure. Body path stability is judged based on the total estimated lateral (sideways) displacement of the robot's path over the length of the test track. If the robot crosses the finish line with an estimated lateral displacement greater than 1 m ( $d > 1$  m), the test is recorded as a steering failure. A run that does not fall into the any of the above categories is considered a successful run. A data set normally consists of a total of 10 runs.

### B. Results

Three sets of 10 trials were performed for forward speed set-points of 0.64, 0.86, and 1.15 m/s. In addition, tests were performed for forward speed set-points of 0.57 and 1.29 m/s to determine the maximum and minimum speeds attainable for the given gait and controller parameters. The mean error in the average speed was 4.3% with a maximum error of 0.05 m/s. Table 3 presents speed error, average power consumption, specific resistance, and repeatability data for tests at 5 different forward speed set-points.

TABLE 3: BASELINE EXPERIMENTAL DATA

| Desired Forward Speed (m/s) | Mean Average Speed (m/s) | Mean Speed Error (%) | Ave. Power Consumed (W) | Mean Specific Resistance, $\epsilon$ | # Trials / Success rate |
|-----------------------------|--------------------------|----------------------|-------------------------|--------------------------------------|-------------------------|
| 0.57                        | 0.61                     | 7.0                  | 78.3                    | 1.55                                 | 1/100%                  |
| 0.64                        | 0.67                     | 4.7                  | 78.9                    | 1.42                                 | 10/100%                 |
| 0.86                        | 0.87                     | 1.2                  | 85.5                    | 1.20                                 | 10/100%                 |
| 1.15                        | 1.07                     | -7.0                 | 94.9                    | 1.07                                 | 10/100%                 |
| 1.29                        | 1.28                     | -2.2                 | 95.7                    | 0.92                                 | 1/100%                  |

Energy efficiency is particularly important in power autonomous mobile robot applications. As a measure of energetic efficiency the *specific resistance* is used [5]. This measure of the energetic cost of locomotion is calculated as

$$\epsilon = \frac{P_{ave}}{mgv_{ave}}, \quad (11)$$

where  $P_{ave}$  is the average total electrical power consumed,  $m$  is the mass of the robot,  $g$  is the gravitational constant, and  $v_{ave}$  is the speed of locomotion. From Table 3, we see that although power consumption increases with forward speed, specific resistance decreases significantly. With different legs and controller parameter values from the above data, the most efficient gait obtained had a specific resistance of 0.9 for a 0.94 m/s forward speed.

A sample plot of instantaneous total electrical power during a 0.89 m/s run is shown in Fig. 7. The power spikes occur around touchdown and lift-off where the moment due to gravity and inertia forces about the foot is largest.

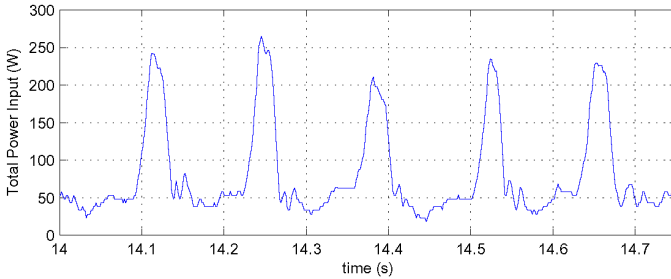


Fig. 7: Total electrical robot power consumption

An additional set of 10 trials was performed for a forward speed set-point of 0.64 m/s under the same conditions as the data in Table 3, but with the steering controller disabled. The estimated lateral displacement,  $d$ , of the robot over the length of the track was used as a measure to test the performance of the steering controller. Using the stability criteria presented previously, 5 of 10 experiments resulted in steering failures, as given in Table 2. This shows the importance of the steering controller. In addition, the steering controller resulted in significantly reduced lateral displacement and less variation in lateral displacement.

Fig. 5 shows stable run data over a 5 m (approx. 0.86 m/s) run. The top plot shows desired and actual body lean ( $\theta - \theta_b$ ) angles. Errors are limited to  $\pm 2^\circ$  most of the time, with occasional  $\pm 3^\circ$  error spikes, indicating that the

TABLE 2: STEERING CONTROLLER DATA

| Steering Enabled | Desired Forward Speed, $v_a$ (m/s) | Mean Lateral Disp., $d$ (m) | Std. Dev. of $d$ (m) | # Trials / Success rate |
|------------------|------------------------------------|-----------------------------|----------------------|-------------------------|
| Yes              | 0.64                               | -0.09                       | 0.24                 | 10 / 100 %              |
| No               | 0.64                               | -0.69                       | 0.87                 | 10 / 50%                |

forward speed is quite sensitive to the lean angle. The bottom plot shows the desired and actual average speeds as well as the estimated forward speed. Both the average actual speed and estimated forward speed show good tracking of the desired speed, with the maximum error in the estimated forward speed being approximately 7%.

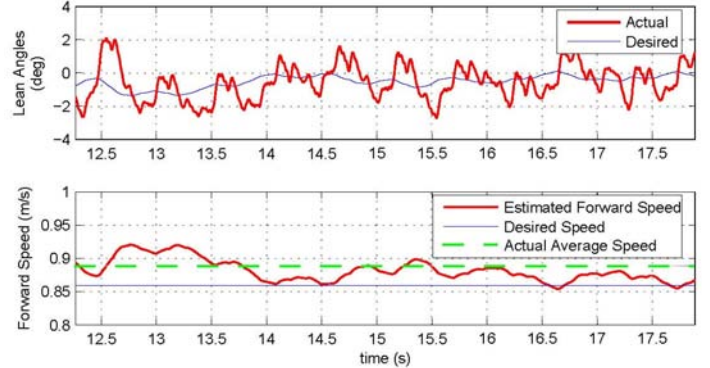


Fig. 5: Top: Typical desired and actual lean angle plots for a 0.89 m/s runs. Bottom: Desired forward speed, estimated forward speed, actual average speed.

Fig. 6 shows the desired and actual leg angles and velocities (top and middle plots) as well the associated estimated motor currents (bottom plot). The position trajectories are offset by  $90^\circ$  due to the ‘‘S’’ shaped legs, and not  $180^\circ$  as in Fig. 4. In addition, the desired trajectories are not as simple or as smooth as in Fig. 4 because the gait parameters are updated every sampling instant to achieve stable biped running. In the plot light shading corresponds to right leg in an assumed single support stance phase, darker shading corresponds to the left leg in an assumed single

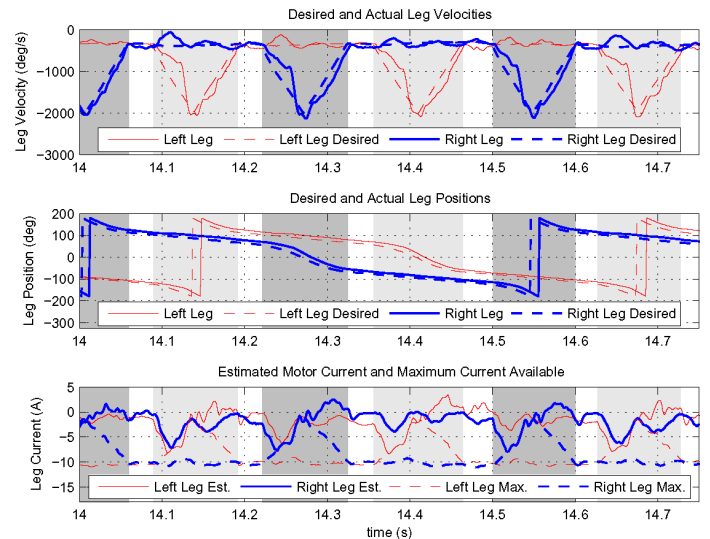


Fig. 6: Leg positions, velocities, and estimated motor currents. Estimated current plot includes the maximum available current for the given speed

support stance phase, and no shading indicates an assumed double support phase. Both the leg position and velocity trajectories exhibit significant errors from the desired values because low tracking gains are used to achieve the desired gait dynamics.

Fig. 8 shows plots of the body roll (top) and yaw (bottom) angles. For relatively small disturbances a (passively) stable small amplitude rolling oscillation is present. Larger disturbances can cause the rolling oscillations to amplify until failure. Stability in the frontal plane was primarily addressed by appropriate duty factor values and by choosing appropriate leg trajectory tracking gains.

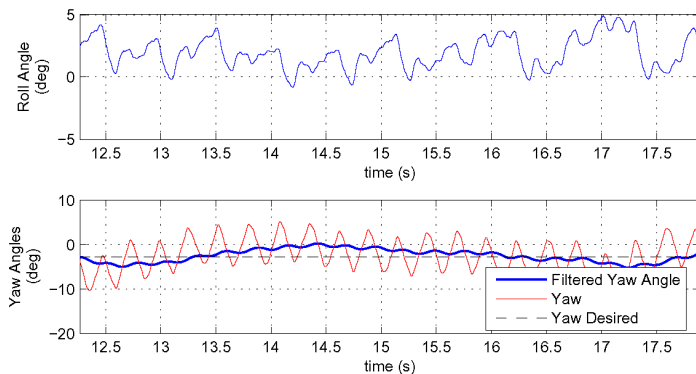


Fig. 8: Top: body roll angle. Bottom: body yaw angle, filtered yaw angle, and desired yaw angle.

A yaw angle oscillation of approximately  $4^\circ$  amplitude is present in the bottom plot of Fig. 8, illustrating the need for the filtered yaw angle in the steering controller. The plot also shows good tracking of the desired straight body path.

## VI. CONCLUSION AND FUTURE WORK

We have demonstrated the first stable bipedal dynamic robot running with one actuator per leg and minimal sensing. Our platform is RHex, a power autonomous, one actuated DOF per leg hexapod, with two-spoked “S” shaped, compliant hind legs. Based on this initial success, further developments could address running with the original single-spoked “C” shaped legs, continuous speed control, steering, and standing up from six-legged to two-legged operation.

## ACKNOWLEDGEMENTS

This work was supported by DARPA/SPAWAR contract N66001-00-C-8026. The authors would like to thank the other RHex project’s Principal Investigators and their local university teams for making this research possible, and for providing a stimulating and supportive research environment – Dr. Koditschek at University of Pennsylvania, Dr. Rizzi at Carnegie Mellon University and in particular Dr. Full at University of California at Berkeley for providing the inspiration for RHex and its bipedal gait, and for many related fascinating discussions. Furthermore, we gratefully acknowledge the help provided by the team members at McGill’s Ambulatory Robotics Lab, in particular to D. McMordie, M. Smith, C. Prahacs, and D. Campbell for

help with various aspects of robot design, maintenance, sensing, data logging and coding. N. Neville would like to thank the Natural Sciences and Engineering Research Council of Canada (NSERC) for their financial support.

## REFERENCES

- [1] R. Blickhan and R.J. Full, “Similarity in multilegged locomotion: bouncing like a monopode”, *J. Comparative Physiology*, vol. A. 173, p. 509-517, 1993.
- [2] D. Campbell and M. Buehler, “Preliminary bounding experiments in a dynamic hexapod”, In B. Siciliano and P. Dario, eds, *Experimental Robotics VIII*, in “Lecture Notes in Control and Information Sciences”, Springer-Verlag, p. 612-621, 2003.
- [3] R.J. Full, K. Autumn, J.I. Chung, and A. Ahn, “Rapid negotiation of rough terrain by the death-head cockroach”, *American Zoologist*, vol. 38, p. 81A, 1998.
- [4] R.J. Full and M.S. Tu, “Mechanics of a rapid running insect: two-, four-, and six-legged locomotion.” *J. Exp. Biology*, 156:215-231, 1991.
- [5] G. Gabrielli and TH. von Karman, “What price speed?”, *Mechanical Engineering*, 775-781, Oct. 1950.
- [6] L. Geppert, “QRIO, the robot that could,” *IEEE Spectrum*, 41(5):34–37, May 2004.
- [7] M. Gienger K. Löffler and F. Pfeiffer, “Sensors and control concept of walking “Johnnie”.” *Int. J. Robotics Research*, 22(3):229–239, March 2003.
- [8] K. Kaneko et al., “Humanoid robot HRP-2”. *IEEE Int. Conf. Robotics and Automation*, p. 1083–1090, April 2004.
- [9] J.-H. Kim and J.-H. Oh, “Realization of dynamic walking for the humanoid robot platform KHR-1,” *Adv Robotics*, 18(7):749–768, August 2004.
- [10] D. McMordie and M. Buehler, “Towards pronking with a hexapod Robot,” *Int. Conf. Climbing and Walking Robots*, p. 659-666, 2001.
- [11] E.Z. Moore and M. Buehler, “Stable stair climbing in a simple hexapod”, *Int. Conf. Climbing and Walking Robots*, p. 603-610, 2001.
- [12] E.Z. Moore, D. Campbell, F. Grimmering and M. Buehler, “Reliable stair climbing in the simple hexapod ‘RHex’”, *IEEE Int. Conf. Robotics and Automation*, p. 2222-2227, 2002.
- [13] N. Neville, M. Buehler, “Towards Bipedal Running of a Six Legged Robot,” 12th Yale Workshop on Adaptive and Learning Systems, May 2003
- [14] K. Nishiwaki et al., “Design and development of research platform for perception-action integration in humanoid robot: H6”. In *IEEE/RSJ Int. Conf. on Intelligent Robots and Systems*, pp 1559–1564, 2000.
- [15] R. Playter and M. Raibert, “Control of a biped somersault in 3D,” *IEEE/RSJ Int. Conf. on Intelligent Robots and Systems*, p. 582-589, 1992.
- [16] Y. Sakagami et al., “The intelligent ASIMO: system overview and integration,” *IEEE/RSJ Int. Conf. on Intelligent Robots and Systems*, p. 2478- 2483, 2002.
- [17] U. Saranli, M. Buehler and D.E. Koditschek, “RHex: A Simple and Highly Mobile Hexapod Robot,” *Int. J. Robotics Research*, 20(7):616-631, July 2001.
- [18] U. Saranli and D.E. Koditschek, “Back flips with a hexapedal robot,” *IEEE Int. Conf. Robotics and Automation*, p. 2209-2215, 2002.
- [19] Video of 1999 swimming implementation at [www.cim.mcgill.ca/~arlweb](http://www.cim.mcgill.ca/~arlweb) and [www.rhex.net](http://www.rhex.net).